microarray expression analysis. Skeletal muscle samples from four FCMD patients and one MDC1A patient were obtained via biopsy at various ages during childhood (Fig. 1). In all CMD samples, histological examination revealed dystrophic features and marked variations in fiber size with less evidence of severe necrotic and regenerating fibers, prominent interstitial tissues, and adipose tissue proliferation (Fig. 1A, F1–F4, M1).

Abundant interstitial tissue was the most characteristic feature in all samples, appearing as early as 20 days of age (Fig. 1A, F1). To quantify the extent of interstitial tissue, we measured the areas of muscle, lipid, and

Table 2a
Genes up-regulated in both FCMD and MDC1A skeletal muscle

Genbank Nos.	Product	Common name	Fold change	
			FCMD	MDC1A
Muscle components				
NM_005159	Actin, α, cardiac muscle precursor	*ACTA*	5.1	8.3
NM_004997	Myosin-binding protein H	*MYBPH*	9.4	6.7
NM_003063	Sarcolipin	*SLN*	9.1	9.6
NM_005022	Profilin 1	*PFN1*	6.6	4.5
XM_010544	*N*-Acetylgalactosaminyltransferase 7	*GALNT7*	6.5	9.5
NM_003186	Transgelin	*TAGLN*	4.2	8.7
NM_001614	Actin, γ1 propeptide	*ACTG*	5.8	8.6
NM_004393	Dystroglycan 1 precursor	*DAG1*	1.5	1.6
ECM components				
NM_000090	α1 type III collagen preproprotein	*COL3A1*	50.1	54.6
NM_003248	Thrombospondin 4	*THBS4*	50	154.6
NM_006475	Osteoblast-specific factor 2	*OSF-2*	20.3	28.1
NM_003380	Vimentin	*VIM*	13.5	18.2
NM_002295	Laminin receptor-1 (67kD)	*LAMR1*	12.3	5.4
NM_003118	Osteonectin	*SPARC*	11.9	26.5
M55270	Matrix Glia protein	*MGP*	11.4	7.3
XM_045926	Lumican	*LUM*	11.2	31.9
NM_002727	Proteoglycan 1, secretory granule	*PRG1*	5.2	4.0
NM_005507	Cofilin 1 (non-muscle)	*CFL1*	4.6	5.7
NM_005410	Selenoprotein P precursor	*SEPP1*	4.5	4.6
NM_002292	Laminin, β 2 precursor	*LAMB2*	3.3	2.2
NM_000426	Laminin, α-2 (merosin)	*LAMA2*	2.9	0.8
NM_000419	Integrin β 1 (fibronectin receptor)	*ITGB1*	2.9	4.2
NM_032470	Tenascin XB, isoform 2	*TNXB*	2.7	6.5
Cell differentiation and adhesion				
X02508	Acetylcholine receptor (AChR) α subunit	*ACHR*	25.9	20.2
NM_000041	Apolipoprotein E	*APOE*	14.8	8
NM_000079	Cholinergic receptor, nicotinic, α precursor	*CHRNA1*	11.3	7.3
NM_002970	Spermidine/spermine N1-acetyltransferase	*SAT*	8.9	11.6
NM_001553	Insulin-like growth factor binding protein 7	*IGFBP7*	7.4	6.8
AF144103	NJAC protein	*NJAC*	2.8	4.3
NM_002402	Mesoderm-specific transcript (mouse) homolog	*MEST*	5.6	6.1
NM_000919	Peptidylglycine α-amidating monooxygenase	*PAM*	5.5	10.8
NM_000700	Annexin I	*ANXA1*	5.1	11.6
NM_001129	Adipocyte enhancer binding protein 1	*AEBP1*	3.8	21.3
Immune related				
M27635	Lymphocyte antigen	*HLA-DRw12*	10.2	3.6
NM_022555	Major histocompatibility complex	*HLA-DRB3*	10.1	3.9
Others, EST				
L01124	Ribosomal protein S13	*RPS13*	6.5	8.1
BC005863	Ribosomal protein, large, P0	*RPP0*	6.3	4.6
NM_00597	Calcium-binding protein A13	*S100A13*	5.2	6.2
NM_006000	Tubulin, α1	*Tuba1*	5	6.1
EST				
AL049455	Unknown	*dkfzp586d2322*	4.4	17.2
AL038078	Unknown	*dkfzp566k121*	7.2	9.8
Glycosyltransferase				
NM_018446	Glycosyltransferase AD-017	*AD-017*	1.5	2.8
XM_003527	*N*-Acetylgalactosaminyltransferase 7	*GalNac*	1.9	2.3
NM_005827	UDP-galactose transporter related	*UGTREL1*	1.3	1.3

connective tissue in each sample specimen using Scion Image (Fig. 1B). The relative area of interstitial tissues varied but did not correlate with patient age. Inflammation and regeneration were less apparent. In all samples examined, necrotic fibers were rare compared with DMD (Fig. 1A, D1). It is noteworthy that necrotic lesions are the least severe in F1 despite the abundance of interstitial tissue.

Next, we measured the cross-sectioned diameter of each muscle fiber. Diameters of FCMD and MDC1A muscle fibers are significantly smaller than those of normal sample fibers at 7 months of age (Fig. 1A, C1, and C; Student's t test, $p < 0.005$). Size variability among muscle fibers was remarkable in the CMDs (Fig. 1C). Some fibers were too thin to analyze, indicating immature, poor muscle components. In contrast, DMD muscle fibers exhibited degeneration and necrosis of muscle fibers accompanied by active regeneration (Fig. 1A, D1). These observations suggest that active regeneration and degeneration, which are characteristic of classical muscular dystrophies, might not be a primary feature of FCMD and MDC1A.

Overall gene expression profiles are highly similar among CMDs, regardless of pathological changes

We analyzed gene expression profiles of CMD skeletal muscle and normal controls to assess the correlation of histological features with gene expression. Scatter graphs of expression data were created for general comparison of expression profiles. The lack of concordance between FCMD and control data indicates the altered expression of numerous genes in disease muscle (Fig. 2A). In contrast, comparison of any two FCMD samples showed good concordance (Fig. 2B), and we observed high correlation among all FCMD cases regardless of pathological differences. We then calculated the correlation co-efficiency of microarray data among FCMD, MDC1A, and normal

Table 2b
Genes down-regulated in both FCMD and MDC1A skeletal muscle

Genbank Nos.	Product	Common name	Fold change	
			FCMD	MDC1A
Muscle components				
NM_000257	Myosin, heavy polypeptide 7, cardiac muscle, β	*MYH7*	0.01	0.01
NM_003673	Titin-cap (telethonin)	*TCAP*	0.02	0.01
NM_001927	Desmin	*DES*	0.01	0.02
NM_017534	Myosin, heavy polypeptide 2, skeletal muscle, adult	*MYH2*	0.02	0.01
NM_005963	Myosin-binding protein C, fast-type	*MYH1*	0.02	0.01
NM_000232	Sarcoglycan, β	*SGCB*	0.03	0.05
NM_001103	Actinin, α2	*ACTN2*	0.04	0.02
NM_004533	Myosin-binding protein C, fast-type	*MYBPC2*	0.09	0.03
NM_003283	Troponin T1, skeletal, slow	*TNNT1*	0.32	0.5
NM_001100	α1 actin precursor	*ACTA1*	0.06	0.03
X04201	Skeletal muscle tropomyosin	*AA 1-285*	0.14	0.31
Cell differentiation and adhesion				
NM_001958	Eukaryotic translation elongation factor 1 α 2	*EEF1a2*	0.03	0.01
NM_002654	Pyruvate kinase, muscle	*PKM2*	0.05	0.02
NM_053013	Enolase 3	*ENO3*	0.09	0.03
NM_000237	Lipoprotein lipase precursor	*LPL*	0.18	0.45
BC007810	Calpain 3, (p94)	*CALP 3*	0.17	0.12
Energy metabolism				
NM_001824	Creatine kinase, muscle	*CKM*	0.12	0.05
NM_000034	Aldolase A	*ALDOA*	0.21	0.07
NM_004320	ATPase, Ca^{++} transporting, fast twitch 1	*ATP2a1*	0.19	0.05
Others, EST				
NM_016172	Putative glialblastoma cell differentiation-related	*GDBR1*	0.21	0.1
NM_004468	Four and a half LIM domains 3	*FHL3*	0.05	0.03
NM_001449	Four and a half LIM domains 1	*FHL1*	0.07	0.07
NM_005053	RAD23 (*Saccharomyces cerevisiae*) homolog A	*RAD23a*	0.08	0.03
NM_004305	Bridging integrator 1	*BIN1*	0.11	0.05
J03077	Human co-β glucosidase	*Glba*	0.09	0.04
XM_054526	Z-band alternatively spliced PDZ-motif	*ZASP*	0.12	0.09
XM_058642	Similar to adenylosuccinate synthetase	*loc122622*	0.13	0.09
XM_035635	Hypothetical protein DKFZp762M136	*dkfzp762M136*	0.13	0.09
NM_005061	Ribosomal protein L3-like	*RPL31*	0.13	0.17
AA164729	Similar to contains Alu repetitive element	*PTR5*	0.13	0.22
AW755254	Similar to CMYA5 Cardiomyopathy associated gene 5	*CMYA5*	0.2	0.15
XM_034768	Hypothetical protein XP_034768	*PDE4DIP*	0.21	0.18

Table 3a.
Selected genes discerning expression in FCMD and MDC1A versus normal muscle

Genbank Nos.	Common	Product
FCMD and MDC1A specific genes		
Up-regulated		
X02508	*ACHR*	Acetylcholine receptor (AChR) α subunit
NM_000090	*COL3a1*	α1 type III collagen preproprotein
NM_000079	*CHRNA1*	Cholinergic receptor, nicotinic, α polypeptide 1 (muscle)
NM_003248	*THBS4*	Thrombospondin 4
NM_003380	*VIM*	Vimentin
XM_049131	*TRA1*	Hypothetical protein XP_049131
NM_005507	*CFL1*	Cofilin 1 (non-muscle)
NM_000041	*APOE*	Apolipoprotein E
NM_003186	*TAGLN*	Transgelin
L01124	*RPS13*	Ribosomal protein S13
NM_004615	*TM4SF2*	Transmembrane 4 superfamily member 2
NM_004997	*MYBPH*	Myosin-binding protein H
Down-regulated		
NM_000232	*SGCB*	Sarcoglycan, β (43kD dystrophin-associated glycoprotein)
NM_003673	*TCAP*	Titin-cap (telethonin)
NM_031287	*MGC3133*	Hypothetical protein MGC3133
NM_000382	*ALDH3a2*	Aldehyde dehydrogenase 3A2
NM_015994	*ATP6m*	Vacuolar proton pump delta polypeptide
NM_014944	*KIAA0911*	KIAA0911 protein
NM_013383	*TCFL4*	MAX-like bHLHZIP protein
NM_004468	*FHL3*	Four and a half LIM domains 3

controls. Any two paired samples showed high correlation co-efficiency (Table 1). The upper right columns indicate the correlation of the actual fold increase or decrease data (Pearson's correlation) and the lower left columns represent the ranking of fold change data (Spearman's correlation). Correlation coefficients for each average fold ratio and the ranking score between F1–F4 and M1 were as high as 0.91 and 0.86, respectively (Table 1, Fig. 2C). These data demonstrate that overall gene expression in these CMDs is similar regardless of age difference, pathological change or type of CMD.

Expression of ECM-related genes is highly elevated, whereas that of mature muscle components is down-regulated in CMDs

Differentially expressed genes were categorized by the function of the encoded protein according to the Gene Ontology classification (e.g., muscle component, ECM component, cell adhesion and growth, inflammation, cellular metabolism, immune response, EST, etc.). For all four CMD individuals, the average ratio of normalized signal intensities relative to normal controls was estimated as a fold change (Tables 2a and 2b).

The vast majority of up-regulated genes in FCMD and MDC1A encode ECM components (Table 2a). This bias is prominent compared to DMD profiles, which show increased expression of genes encoding skeletal muscle components [22]. ECM genes up-regulated in CMDs include *thrombospondin 4*, *collagen3a1*, *collagen15a1*, *osteoblast-specific factor*, *matrix glia protein*, and *lumican* (Table 2a). The high expression of ECM genes presumably is related to fibrotic change, as shown in Fig. 1A. However, expression of fibronectin receptor *integrin 5α*, which is typically up-regulated due to inflammation or fibrosis, showed only a mild increase (1.09 average fold ratio to control in FCMD samples). This observation implies that fibrosis in CMD muscles might result from additional factors to chronic inflammation or muscle fiber degeneration. Genes encoding basement membrane components such as *tenascin*, *laminin receptor-1*, *laminin β*, and *integrin α7* also were up-regulated, as was *DAG1*, which encodes α and β-DG (Table 2a).

Increased expression of the muscle components γ *actin-1*, *myelin basic protein*, *tropomyosin*, and *sarcosin* was observed in the CMDs. Other muscle components, including *myosin heavy chain 2* and *7*, *nebulin*, *titin*, and *desmin*, showed much lower expression levels in CMDs relative to controls (Table 2b). These observations are consistent with previously published expression profiles of DMD muscles [22]. Although some genes encoding components of mature muscle fibers, such as *myosin light chain4* or, *cardiac actinα*, are up-regulated in DMD (Table 4-2, and [22]), these genes were not up-regulated in CMDs. Up-regulation of genes encoding muscle fiber components in DMD generally reflects active regeneration following muscle fiber degeneration. Our observations indicate that muscle degeneration and regeneration are less active in CMDs. Moreover, genes related to cell metabolism, such as *phosphofurkutokinase* and *aldolase*, were substantially down-regulated, suggesting that the total energy metabolism in CMD muscle fibers is likely reduced (Table 2b).

In summary, expression profiling revealed two characteristics. First, most up-regulated genes were ECM

components that may be related to rich interstitial tissues in CMDs. Second, mature muscle components were extremely down-regulated in CMDs. Our data are consistent with the histological finding that the primary feature of CMDs is interstitial fibrosis without muscle degeneration and regeneration.

The Distillation extracted up-regulated ECM genes and suppressed muscle structural genes in CMDs

Bioinformatics using multi-dimensional analysis allowed detection of gene clusters whose expression patterns might help explain CMD pathogenesis [24,25]. We adopted an original statistical analysis method, the Distillation, to extract genes whose expression signals significantly distinguish FCMD, MDC1A, and normal skeletal muscle [23]. Using this method, genes were extracted either as a single gene or as paired genes showing significant expression tendencies between samples tested.

We first analyzed microarray data for genes that distinguish the CMD samples from normal skeletal muscle. From 2345 genes tested, 20 genes were extracted (Table 3a). These include *achr*, *col3a1*, and *thbs4*, which were up-regulated in CMDs. β-Sarcoglycan and *telethonin*, which encode mature muscle components, were down-regulated (Fig. 3A).

Next, we extracted 20 genes that distinguish FCMD from MDC1A and normal controls (Table 3b). Up-regulated genes within this group included *hla-drw1*, *hla-drb3 TNNT-2*, and *lamα2*. In addition, 10 genes paired with *MYH7* were extracted, nine of which have unknown functions (Table 3b). When signals for these pairs are plotted on two-dimensional graphs, distinct expression tendencies become apparent within each disease group (Fig. 3B). These genes might be functionally linked to *MYH7* and contribute to molecular mechanisms underlying FCMD. *CGI-38 brain-specific protein* of unknown function was selected since its expression in MDC1A is distinct from other groups. Nine genes, including *myogenin* and *thyroid hormone binding protein*, were extracted in pair with *CGI-38* (Table 3c).

To find genes specifically involved in these CMDs compared to classical muscular dystrophy, we compared FCMD expression profiles with previously reported DMD profiles [22]. Genes including *chnra, thsb4*, *col3a*, *col15a1*, and *hla-drw12* (Table 4a) were found to be up-regulated in FCMDs and down-regulated in DMD. The genes *actc2*, *actg1 MYH7, MYH2*, and *MYH1* (Table 4b) were down-regulated in FCMD and up-regulated in DMD. These results corroborate the general finding that genes up-regulated in FCMD are mainly ECM components, whereas down-regulated genes tend to be muscle components, differentiating FCMD from DMD.

To confirm the microarray data, we performed real-time quantitative PCR for several selected genes extracted by the Distillation (Figs. 4A and B). This experiment replicated the distinct gene expression patterns seen in CMDs

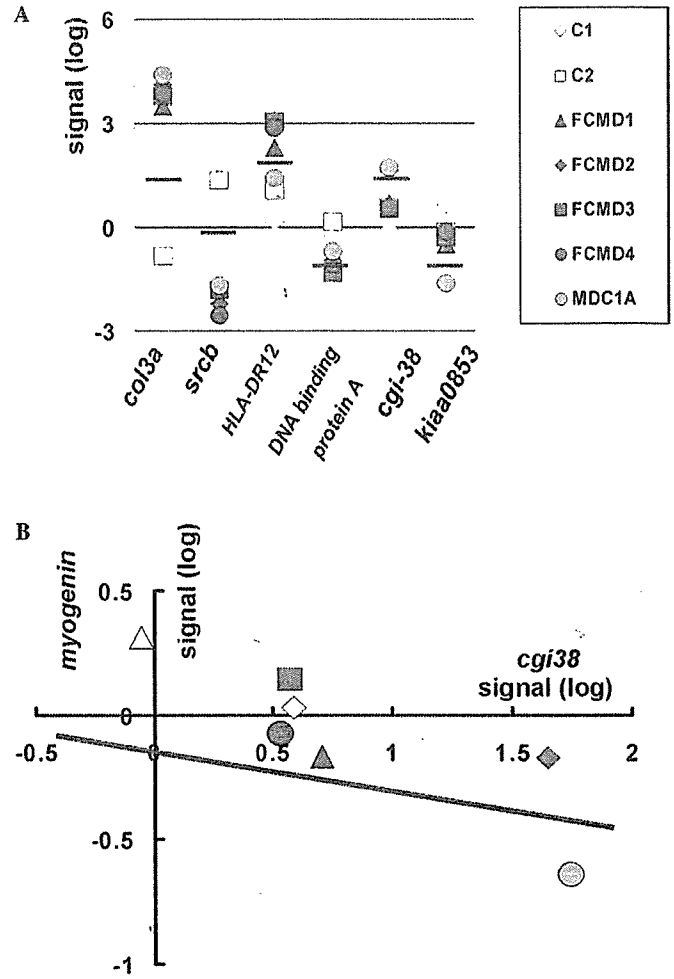

Fig. 3. The Distillation. (A) Several genes sorting FCMD, MDC1A, and normal controls are selected (blue lines). The vertical line shows log scaled signal expression for each gene. *Col3a* and *srcβ* are isolated in the expression profiles of FCMD and MDC1A versus normal control muscle. *HLADR12* and *DNA binding protein A* also discern FCMD from MDC1A and normal muscle; likewise, *CGI-38* and *kiaa 0853* show distinct expression patterns in MDC1A compared to FCMD and normal control. (B) Paired genes sorting FCMD and MDC1A from normal muscle. The horizontal line shows log scaled signal expression of *CGI-38*, and the vertical line shows signal expression of *myogenin*. Note that expression signals of these genes two-dimensionally separate disease groups, suggesting the possibility of linked interactions between these genes.

compared to DMD or normal muscle, demonstrating the reliability of the Distillation as well as the microarray analysis itself. Therefore, these extracted genes likely reflect the unique features of FCMD and MDC1A.

Characteristics of CMDs include elevated expression of muscle cell ECM components

FCMD gene expression profiles were quite similar regardless of age differences or muscle pathology among samples. Since muscle content and fibrotic components vary among patients, we normalized gene expression signals by dividing each signal by the gross area of each muscle component according to the data in Fig. 1B. When

signals in different stages of FCMD were proportionally normalized, gene expression patterns of muscle components such as *myosin light chain 1* and *actin* γ stabilized across samples F1–F4 (Fig. 5). Genes related to muscle fiber components in FCMD seem to be stably expressed irrelevant of muscle fiber content. On the other hand, normalizing expression in FCMD relative to the gross area of interstitial tissue did not stabilize the tendency toward ECM component expression, suggesting that expression of ECM genes does not correlate proportionally with the severity of fibrotic change (Fig. 5). These results imply that expression of fibrotic components in FCMD might not arise from dystrophic change but instead is related to muscle component expression. The high and stable expression of ECM components among all samples indicates that fibrosis is active from very early infancy and may last throughout the disease course.

To clarify which cells express ECM components in FCMD muscles, in situ hybridization was performed for the up-regulated ECM genes *col3a*, *col15a1*, *OSF-2*, and *thbs4*. Surprisingly, these components were expressed primarily by muscle fibers in FCMD, particularly from small-sized, immature muscle cells and satellite cells (Fig. 6), and only slightly by fibroblasts within fibrous tissue. This suggests that the fibrotic change in CMDs is a primary phenotype rather than a secondary effect of chronic inflammation, as is seen in classical muscular dystrophy. Taken together, these results indicate that FCMD and MDC1A can be characterized as active fibrotic disease with suppressed muscle regeneration.

Discussion

Extraction of disease determinant genes using the Distillation

Analysis of gene expression in various tissues or cell samples has evolved from assessment of select target genes to more efficient, high-throughput genomewide screening. Microarray technology can provide valuable insight into important biological and pathological mechanisms and aid in identifying disease-causing genes [25,26]. However, the most emergent challenge in microarray analysis is separating valid data from the 'noise' that inevitably exists in the vast amount of redundant data produced by high-throughput screening. If genes identified through microarray analysis have a true correlation, determining what is statistically 'not true' is another issue. Bioinformatics has made it possible to address such problems by isolating statistically distinct genes [23]. The Distillation (also called TidalSMP, [23]) is a proven method for sorting reliable disease-specific genes using an original, efficient algorithm for mining association rules to determine a correlation.

The dystrophin–glycoprotein complex is a multi-subunit complex, comprised of sarcoplasmic and integral

Table 3b
Selected genes discerning expression in FCMD versus MDC1A and normal muscle

Genbank	Common	Product
FCMD-specific genes		
Up-regulated		
M27635	*HLA-drw12*	Lymphocyte antigen
NM_022555	*HLA-drb3*	Major histocompatibility complex, class II, DR β 3
XM_009540	*KIAA0255*	KIAA0255 gene product
NM_000364	*TNNT2*	Troponin T2, cardiac
NM_000237	*LPL*	Lipoprotein lipase precursor
NM_000426	*Lama2a*	Laminin, α-2 (merosin)
Down-regulated		
NM_000257	*MYH7*	Myosin, heavy polypeptide 7, cardiac muscle, beta
L29073	*EST*	DNA-binding protein a
AL043327	*DKFZP434o1923*	
XM_035662	*LOC137597*	Similar to cathepsin B (H. sapiens)
Down-regulated paired genes		
NM_000257	*MYH7*	Myosin, heavy polypeptide 7, cardiac muscle, beta
and		
NM_017751	*flj20297*	
AF126008	*BRX*	Hypothetical protein FLJ20297
XM_044630	*DKFZP434c131*	Breast cancer nuclear receptor-binding auxiliary protein
BM458054	*EST*	DKFZP434C131 protein
AL157455	*DKFZP761i1912*	IMAGE:553039
XM_042323	*KIAA0833*	EST
NM_014815	*KIAA0130*	KIAA0833 protein
AI401562	*EST*	KIAA0130 gene product
XM_001928	*LOC55924*	IMAGE:2110120
NM_005206	*CRK*	Hypothetical protein

Table 3c
Selected genes discerning expression in MDC1A versus FCMD and normal muscle

Genbank Nos.	Common	Product
MDC1A-specific genes		
Up-regulated		
NM_006471	*MLCB*	Myosin, light polypeptide, non-sarcomeric (20kD)
NM_016140	*LOC51673*	CGI-38 brain-specific protein
Down-regulated		
NM_015070	*KIAA0853*	KIAA0853 protein
XM_012618	*MYH2*	Myosin, heavy polypeptide 2, skeletal muscle, adult
BC004541	*IMAGE:3951723*	Unknown (protein for IMAGE:3951723)
NM_000389	*CDKN1a*	Cyclin-dependent kinase inhibitor 1A
BC008069	*SH3-like*	Similar to src homology three and cysteine rich domain
NM_002479	*MYOG*	MYF4; Myogenic factor-4
NM_006813	*PROL2*	Proline rich 2
NM_000690	*ALDH2*	Aldehyde dehydrogenase 2, mitochondrial
XM_058387	*ANK1*	Ankyrin 1, isoform 8
XM_008333	*ACADVL*	Acyl-Coenzyme A dehydrogenase, very long chain precursor
XM_013017	*KIAA0153*	Hypothetical protein XP_013017
U94777	*PYGM*	Muscle glycogen phosphorylase
NM_004543	*NEB*	Nebulin
NM_003637	*itgal0*	Integrin, α 10
Up-regulated	Paired genes	
NM_016140	*LOC51673*	CGI-38 brain-specific protein
Down-regulated, paired with LOC51673		
NM_002479	*MYOG*	Myogenin
NM_001104	*ACTN3*	Skeletal muscle-specific actinin, α 3
NM_015380	*CGI-51*	CGI-51 protein
NM_002826	*QSCN6*	Quiescin Q6
J02783	*P4hb*	Thyroid hormone binding protein precursor
NM_000884	*IMPDH2*	IMP (inosine monophosphate) dehydrogenase 2
NM_013400	*RIP60*	Replication initiation region protein (60kD)
NM_015070	*KIAA0853*	KIAA0853 protein
NM_000257	*MYH7*	Myosin, heavy polypeptide 7, cardiac muscle, beta

Table 4a
Genes up-regulated in FCMD and down-regulated in DMD

Genbank Nos.	Product	Common name	Fold increase	
			FCMD	DMD
XM_005592	Collagen, type XV, α1	*COL15A1*	2.86	0.43
NM_002229	Jun B proto-oncogene (JUNB)	*JUNB*	2.80	0.70
NM_002402	Mesoderm-specific transcript (mouse) homolog (MEST),	*MEST*	2.61	0.53
NM_024416	Osteoglycin (osteoinductive factor, mimecan) (OGN)	*OGN*	2.59	0.43
NM_000090	Collagen, type III, α1	*COL3A1*	2.42	0.29
X64875	Insulin-like growth factor binding protein-3	*IGFBP-3*	2.27	0.85
NM_006475	Osteoblast-specific factor 2 (fasciclin I-like) (OSF-2)	*OSF-2*	2.08	0.14
NM_000079	Cholinergic receptor, nicotinic, α polypeptide 1	*CHRNA1*	2.01	0.64
M27635	MHC HLA-DRw12 allele mRNA, β-1 chain	*HLA-DRW12*	2.01	0.56
NM_001731	B-cell translocation gene 1, anti-proliferative (BTG1)	*BTG1*	1.99	0.56
XM_004063	Early growth response 1 (EGR1)	*EGR1*	1.98	0.65

membrane proteins that link the cytoskeleton to the ECM [27]. This complex is thought to provide mechanical reinforcement for the sarcolemma and to maintain membrane integrity during cycles of muscle contraction and relaxation. It is known that DG spans the sarcolemma, linking extracellular laminin-α2 with dystrophin/cytoskeleton [17]. Defects in this linkage cause muscular dystrophies, as seen in FCMD and MDC1A [4,5,28]. In this sense, the molecular mechanisms underlying FCMD and MDC1A should be similar. Indeed, gene expression profiles in these disorders are virtually the same. However, using the Distillation, we extracted a number of differentially expressed genes, including some with unknown function.

FCMD and MDC1A as primary fibrosis diseases

Upon histological examination, DMD skeletal muscle fibers showed muscle degeneration and active regeneration.

Table 4b
Genes up-regulated in DMD and down-regulated in FCMD

Genbank Nos.	Product	Common name	Fold change	
			FCMD	DMD
NM_001615	Actin, γ2, (ACTG2), mRNA	*ACTG2*	0.45	8.85
NM_001614	Actin, γ1 (ACTG1)	*ACTG1*	0.55	4.42
XM_005368	Protein kinase PKNbeta (pknbeta)	*PKNBETA*	0.91	4.02
NM_005729	Peptidylprolyl isomerase F (cyclophilin F) (PPIF)	*PPIF*	0.77	2.92
NM_000257	Myosin, heavy polypeptide 7, cardiac muscle, β (MYH7)	*MYH7*	0.63	2.82
XM_027916	HP1-BP74 (HP1-BP74)	*HP1-BP74*	0.50	2.74
NM_002476	Myosin, atrial/fetal muscle, light chain; embryonic (MYL4)	*MYL4*	0.48	2.46
NM_001912	Cathepsin L (CTSL)	*CTSL*	0.83	2.13
NM_005963	Myosin heavy chain IIx/d; skeletal muscle, adult (MYH1)	*MYH1*	0.78	1.91
NM_001927	Desmin, (DES)	*DES*	0.72	1.51
NM_001614	MyHC-IIa; MYHas8; MyHC-2A; myosin, heavy polypeptide 2, skeletal muscle, adult (MYH2)	*MYH2*	0.76	1.33

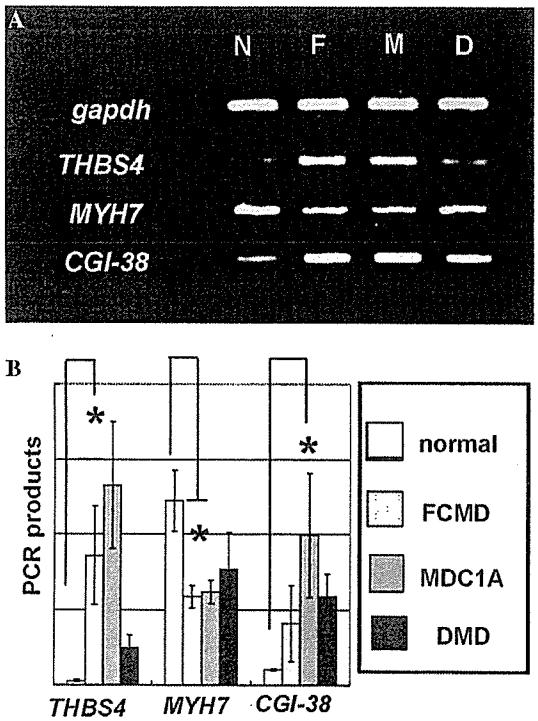

Fig. 4. Gene expression tendencies in CMDs show elevated ECM component expression and low expression of muscle components. (A) Ethidium bromide staining shows up-regulation of *THBS4* and *CGI-38* in FMCD and MDC1A compared to normal muscle and DMD. *MYH7* is down-regulated in FCMD and MDC1A, unlike DMD and normal muscle. (B) Quantitative real-time PCR analysis of mRNA expression. White bar, normal controls; dotted bar, FCMD; gray bar, MDC1A; and black bar, DMD. PCR products are plotted as values normalized to *gapdh*. Each bar represents the mean value of two patients' data. $^*p < 0.005$ (Student's *t* test).

At the molecular level, expression profiling reveals the up-regulation of genes encoding muscle structural proteins, myogenic factors, and immune responses [20,21]. Changes in expression of these genes reflect the clinical phases and histological changes indicating disease progression.

In contrast, our data demonstrate that some of the muscle component genes that are up-regulated in DMD [22] were extremely down-regulated in CMDs. This observation implies less active regeneration of muscle fibers in CMDs. Instead, expression of genes encoding ECM components was substantially high in CMDs. ECM genes are also highly expressed in DMD muscles, generally reflecting a response to necrotic changes in muscle fibers resulting from inflammation. ECM gene expression increases as muscle fibrosis develops due to chronic inflammation at later stages of DMD [22]. In contrast, expression levels of ECM genes in CMD were consistent regardless of histological changes. Further, the elevated ECM genes are not expressed by fibroblasts but by muscle cells themselves. This persistently high expression of ECM genes may be indicative of the primary etiology of CMD.

It has been postulated that dysfunction of *fukutin* in FCMD or laminin-α2 in MDC1A induces severe muscular dystrophy by attenuating stable connections between the skeletal muscle sarcoplasmic membrane and the basement membrane. Indeed, defects in the basement membrane have been reported in FCMD muscle [29]. Basement membrane is thought to not only maintain cell integrity but also to mediate signal transmission in cell differentiation, growth, attachment, survival, polarity, proliferation, and apoptosis [30–32]. We hypothesize that up-regulation of ECM genes observed in these experiments might arise from signal transduction defects due to basement membrane dysfunction.

Regarding the histological characteristics of CMD muscle, one possible explanation for disease etiology is apoptosis of muscle cells. Laminin-α2 is required for myotube survival in vitro [31], and increased apoptotic cells cause embryonic lethality in *fukutin*-null mice due to aberrant basement membrane formation [33]. These findings indicate that the basement membrane is essential to cell survival. Reduction of α-DG in myotubes in vitro also results in reduced levels of laminin expression on cell surfaces and an increase in apoptotic cell death [34]. Hence in normal conditions, connection of laminin and α-DG might be involved in skeletal muscle cell survival. It might be reasonable to imagine that connective tissue simply fills the space created by apoptosis. It is also possible that muscle fibers keeps high transcription levels of ECM to create basement membrane components.

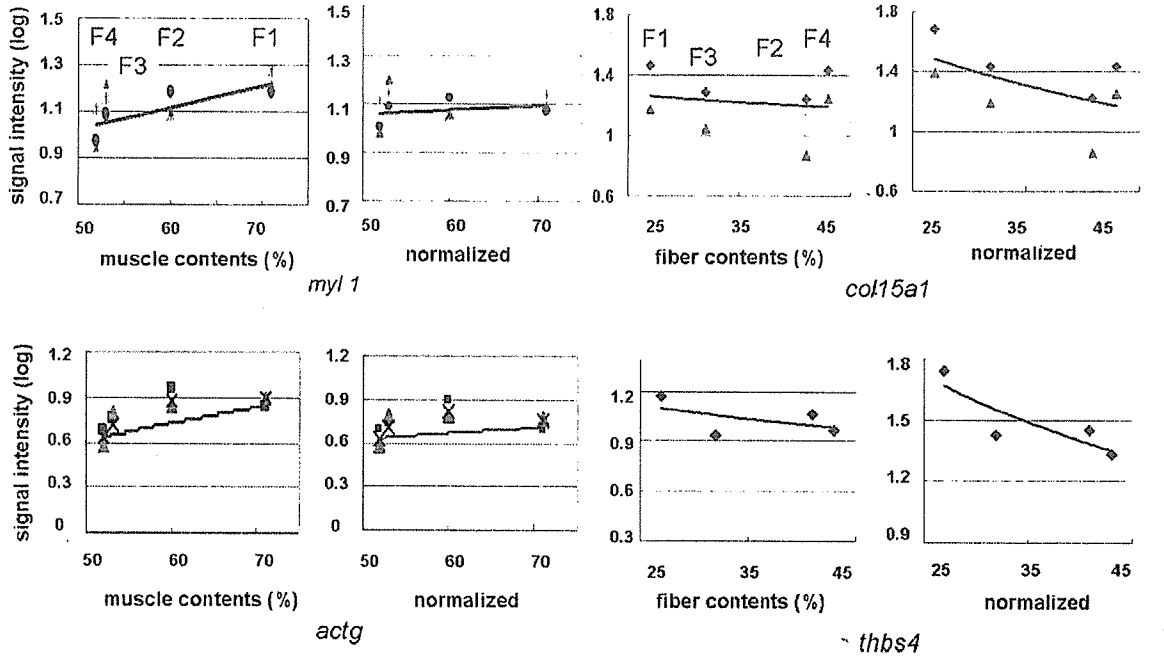

Fig. 5. Gene expression of ECM and muscle component normalized by the area of each component. Each dot shows expression signals of each gene. Each line shows the approximate curves of these signals. *X*-axis, percentage of tissue muscle and interstitial tissue of F1–F4; *Y*-axis, signal intensities of each gene (log scale).

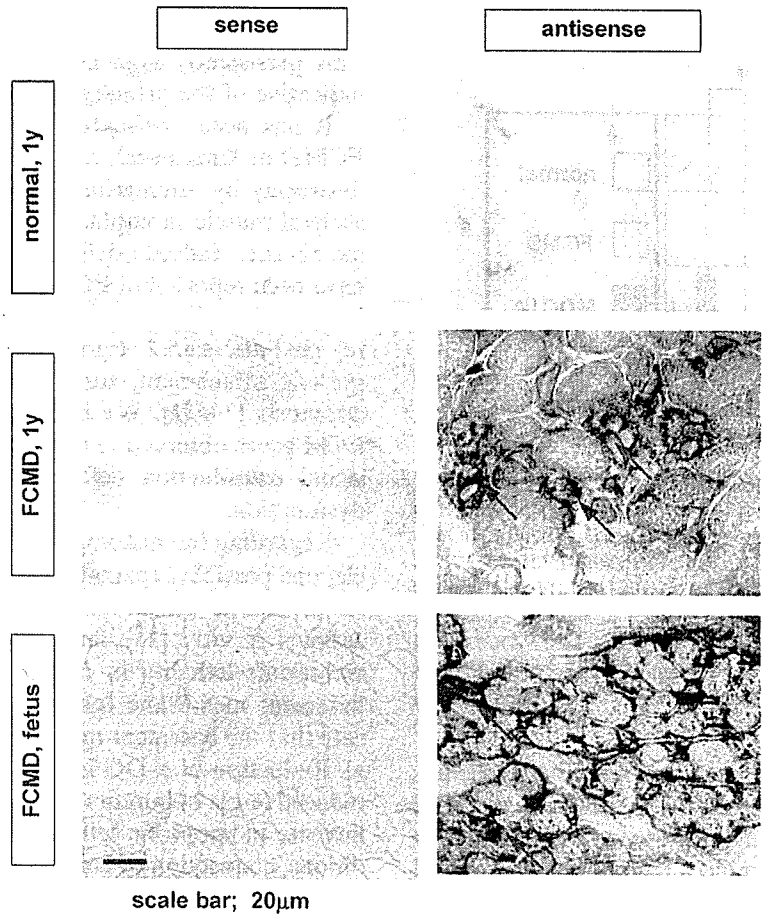

Fig. 6. In situ hybridization of *THBS4* in FCMD skeletal muscle versus normal controls. Upper columns show normal skeletal muscle fibers (1 year of age). No significant *THBS4* signals are seen in muscle fibers (upper right column). Middle columns show FCMD muscle fibers (1 year of age). Bottom columns show fetal (19 weeks) FCMD skeletal muscle. Note that skeletal muscle fibers with small muscle diameters stain positively (arrows) both in FCMD and in fetal tissue (middle and lower right columns). *Col3a*, *col15a*, and *OSF2* show the same results (data not shown). Note that immature muscle fibers, not fibroblasts, express ECM components at high levels.

Alternatively, the differentiation defect in muscle cells might underlie the etiology of these CMDs. Skeletal muscle fibers in FCMD are generally very small, round, and disorganized. Most muscle fibers in CMDs remain small and disorganized with remarkable size diversity. In contrast, regenerating DMD muscle fibers never fail to achieve normal fiber sizes. Skeletal muscle fibers in FCMD somewhat resemble those in fetal skeletal muscle ([35] and unpublished data). Fetal muscle is characterized by premature, small muscle fibers with a high nucleus-to-cytoplasm ratio, rather rich in cell-to-cell intervals with loose muscle bundles. FCMD and MDC1A skeletal muscle fibers might also be in the developmental period of myotubes and muscle fibers, which have substantial space for interstitial ECM components. ECM genes could be up-regulated to promote differentiation of immature muscle cells. It is possible that the delay in differentiation due to the basement membrane defect is significant in the etiology of the CMDs. We presume that maturational arrest is a key factor, followed by up-regulation of ECM components. We have also found neuromuscular junction abnormalities in FCMD (unpublished data) as also have been seen in MDC1A [36]. Since neuromuscular junction formation normally occurs in tandem with basement membrane formation, nerve innervations may also play an important role in muscle differentiation (unpublished data).

Taken together, our observations suggest that the fibrotic change seen in CMDs reflects a primary fibrosis disease rather than the secondary change, as is seen in classical muscular dystrophy. The causes for up-regulation of ECM genes in FCMD and MDC1A muscle merit further scrutiny and may reveal more precise mechanisms for FCMD and MDC1A.

Acknowledgments

We are grateful to Dr. Ikuya Nonaka and Dr. Shin'ichi Takeda for their critical comments and advice, and Dr. Hidetoshi Taniguchi and Dr. Masako Taniike for technical support. We also thank Dr. Jennifer Logan for editing the manuscript. This work was supported by a Health Science Research Grant, Research on Psychiatric and Neurological Diseases and Mental Health and by a Research Grant for Nervous and Mental Disorders (14B-4 and 17A-10), both from the ministry of Health, Labor and Welfare of Japan; and by the 21st Century COE program from the Ministry of Education, Culture, Sports, Science, and Technology of Japan.

References

[1] Y. Fukuyama, M. Osawa, H. Suzuki, Congenital progressive muscular dystrophy of the Fukuyama type-clinical, genetic, and pathological considerations, Brain Dev. 3 (1981) 1–29.

[2] T. Toda, M. Segawa, Y. Nomura, I. Nonaka, K. Masuda, T. Ishihara, M. Suzuki, I. Tomita, Y. Origuchi, K. Ohno, N. Misugi, Y. Sasaki, K. Takada, M. Kawai, K. Otani, T. Murakami, K. Saito, Y. Fukuyama, T. Shimizu, I. Kanazawa, Y. Nakamura, Localization of a gene for Fukuyama type congenital muscular dystrophy to chromosome 9q31–33, Nat. Genet. 3 (1993) 283–286.

[3] K. Kobayashi, Y. Nakahori, M. Miyake, K. Matsumura, E. Kondo-Iida, Y. Nomura, M. Segawa, M. Yoshioka, K. Saito, M. Osawa, K. Hamano, Y. Sakakihara, I. Nonaka, Y. Nakagome, I. Kanazawa, Y. Nakamura, K. Tokunaga, T. Toda, An ancient retrotransposal insertion causes Fukuyama-type congenital muscular dystrophy, Nature 394 (1998) 388–392.

[4] Y.K. Hayashi, M. Ogawa, K. Tagawa, S. Noguchi, T. Ishihara, I. Nonaka, K. Arahata, Selective deficiency of alpha-dystroglycan in Fukuyama-type congenital muscular dystrophy, Neurology 57 (2001) 115–121.

[5] D. Michele, E.R. Barresi, M. Kanagawa, F. Saito, R.D. Cohn, J.S. Satz, J. Dollar, I. Nishino, R.I. Kelley, H. Somer, V. Straub, K.D. Mathews, S.A. Moore, K.P. Campbell, Post-translational disruption of dystroglycan-ligand interactions in congenital muscular dystrophies, Nature 418 (2002) 417–422.

[6] P.K. Grewal, J.E. Hewitt, Glycosylation defects: a new mechanism for muscular dystrophy? Hum. Mol. Genet. 12 (2003) 259–264.

[7] F. Muntoni, M. Brockington, D.J. Blake, S. Torelli, S.C. Brown, Defective glycosylation in muscular dystrophy, Lancet 360 (2002) 1419–1421.

[8] A. Yoshida, K. Kobayashi, H. Manya, K. Taniguchi, H. Kano, M. Mizuno, T. Inazu, H. Mitsuhash, S. Takahashi, M. Takeuchi, R. Herrmann, V. Straub, B. Talim, T. Voit, H. Topaloglu, T. Toda, T. Endo, Muscular dystrophy and neuronal migration disorder caused by mutations in a glycosyltransferase, POMGnT1, Dev. Cell 1 (2001) 717–774.

[9] D. Beltrán-Valero de Bernabé, S. Currier, A. Steinbrecher, J. Celli, E. van Beusekom, B. van der Zwaag, H. Kayserili, L. Merlini, D. Chitayat, W.B. Dobyns, B. Cormand, A. Lehesjoki, J. Cruces, T. Voit, C.A. Walsh, H. van Bokhoven, H.G. Brunner, Mutations in the *O*-mannosyltransferase gene POMT1 give rise to the severe neuronal migration disorder Walker–Warburg syndrome, Am. J. Hum. Genet. 71 (2002) 1033–1034.

[10] J. van Reeuwijk, M. Janssen, C. van den Elzen, D. Beltran-Valero de Bernabé, P. Sabatelli, L. Merlini, M. Boon, H. Scheffer, M. Brockington, F. Muntoni, M.A. Huynen, A. Verrips, C.A. Walsh, P.G. Barth, H.G. Brunner, H. van Bokhoven, POMT2 mutations cause alpha-dystroglycan hypoglycosylation and Walker Warburg syndrome, J. Med. Genet. 12 (2005) 907–912.

[11] M. Brockington, D.J. Blake, P. Prandini, Mutations in the fukutin-related protein gene (FKRP) cause a form of congenital muscular dystrophy with secondary laminin alpha2 deficiency and abnormal glycosylation of alpha-dystroglycan, Am. J. Hum. Genet. 6 (2001) 1198–1209.

[12] C. Longman, M. Brockington, S. Torelli, C. Jimenez-Mallebrera, C. Kennedy, N. Khalil, L. Feng, R.K. Saran, T. Voit, L. Merlini, C.A. Sewry, S.C. Brown, F. Muntoni, Mutations in the human LARGE gene cause MDC1D, a novel form of congenital muscular dystrophy with severe mental retardation and abnormal glycosylation of alpha-dystroglycan, Hum. Mol. Genet. 12 (2003) 2853–2861.

[13] P.K. Grewal, P.J. Holzfeind, R.E. Bittner, J.E. Hewitt, Mutant glycosyltransferase and altered glycosylation of alpha-dystroglycan in the myodystrophy mouse, Nat. Genet. 28 (2001) 151–154.

[14] F.M. Tome, T. Evangelista, A. Leclerc, Y. Sunada, E. Manole, B. Estournet, A. Barois, K.P. Campbell, M. Fardeau, Congenital muscular dystrophy with merosin deficiency, C.R. Acad. Sci. III 317 (1994) 351–357.

[15] A. Helbling-Leclerc, X. Zhang, H. Topaloglu, C. Cruaud, F. Tesson, J. Weissenbach, F.M. Tomé, K. Schwartz, M. Fardeau, K. Tryggvason, P. Guicheney, Mutations in the laminin alpha 2-chain gene (LAMA2) cause merosin-deficient congenital muscular dystrophy, Nat. Genet. 11 (1995) 216–218.

[16] H. Colognato, D.A. Winkelmann, P.S. Yurchenco, Laminin polymerization induces a receptor-cytoskeleton network, J. Cell Biol. 145 (1999) 619–631.

[17] O. Ibraghimov-Beskrovnaya, J.M. Ervasti, C.J. Leveille, C.A. Slaughter, S.W. Sernett, K.P. Campbell, Primary structure of dystrophin-associated glycoproteins linking dystrophin to the extracellular matrix, Nature 355 (1992) 696–702.
[18] J.M. Ervasti, K.P. Campbell, A role for the dystrophin–glycoprotein complex as a transmembrane linker between laminin and actin, J. Cell Biol. 122 (1993) 809–823.
[19] I. Nonaka, H. Sugita, K. Takada, K. Kumagai, Muscle histochemistry in congenital muscular dystrophy with central nervous system involvement, Muscle Nerve 5 (1982) 102–106.
[20] Y.W. Chen, P. Zhao, R. Borup, E.P. Hoffman, Expression profiling in the muscular dystrophies: identification of novel aspects of molecular pathophysiology, J. Cell Biol. 151 (2000) 1321–1336.
[21] J.N. Haslett, D. Sanoudou, A.T. Kho, R.R. Bennett, S.A. Greenberg, I.S. Kohane, A.H. Beggs, L.M. Kunkel, Gene expression comparison of biopsies from Duchenne muscular dystrophy (DMD) and normal skeletal muscle, Proc. Natl. Acad. Sci. USA 99 (2002) 15000–15005.
[22] S. Noguchi, T. Tsukahara, M. Fujita, R. Kurokawa, M. Tachikawa, T. Toda, A. Tsujimoto, K. Arahata, I. Nishino, cDNA microarray analysis of individual Duchenne muscular dystrophy patients, Hum. Mol. Genet. 12 (2003) 595–600.
[23] J. Sese, S. Morishita, Answering the most correlated N association rules efficiently, Proc. of 6th European Conference on Principles and Practice of Knowledge Discovery in Databases, 2002.
[24] M.Q. Zhang, Large-scale gene expression data analysis: a new challenge to computational biologists, Genome Res. 9 (1999) 681–688.
[25] D.D. Bowtell, Options available—from start to finish—for obtaining expression data by microarray, Nat. Genet. 21 (1999) 25–32.
[26] M. Schena, R.A. Heller, T.P. Theriault, K. Konrad, E. Lachenmeier, R.W. Davis, Microarrays: biotechnology's discovery platform for functional genomics, Trends Biotechnol. 16 (1998) 301–306.
[27] J.M. Ervasti, K.P. Campbell, Membrane organization of the dystrophin–glycoprotein complex, Cell 6 (1991) 1121–1131.
[28] M.D. Henry, K.P. Campbell, A role for dystroglycan in basement membrane assembly, Cell 95 (1998) 859–870.
[29] H. Ishii, Y.K. Hayashi, I. Nonaka, K. Arahata, Electron microscopic examination of basal lamina in Fukuyama congenital muscular dystrophy, Neuromuscul. Disord. 3 (1997) 191–197.
[30] M.W. Cohen, C. Jacobson, E.W. Godfrey, K.P. Campbell, S. Carbonetto, Distribution of alpha-dystroglycan during embryonic nerve-muscle synaptogenesis, J. Cell Biol. 129 (1995) 1093–1101.
[31] P.H. Vachon, F. Loechel, H. Xu, U.M. Wewer, E. Engvall, Merosin and laminin in myogenesis; specific requirement for merosin in myotube stability and survival, J. Cell Biol. 134 (1996) 1483–1497.
[32] J.R. Sanes, The basement membrane/basal lamina of skeletal muscle, J. Biol. Chem. 278 (2003) 12601–12604.
[33] H. Kurahashi, M. Taniguchi, C. Meno, Y. Taniguchi, S. Takeda, M. Horie, H. Otani, T. Toda, Basement membrane fragility underlies embryonic lethality in fukutin-null mice, Neurobiol. Dis. 19 (2005) 208–221.
[34] F. Montanaro, M. Lindenbaum, S. Carbonetto, Alpha-dystroglycan is a laminin receptor involved in extracellular matrix assembly on myotubes and muscle cell viability, J. Cell Biol. 145 (1999) 1325–1340.
[35] H.B. Sarnat, Cerebral dysgenesis and their influence on fetal muscle development, Brain Dev. 8 (1986) 495–499.
[36] P.G. Noakes, M. Gautam, J. Mudd, J.R. Sanes, J.P. Merlie, Aberrant differentiation of neuromuscular junctions in mice lacking s-laminin/laminin beta 2, Nature 16 (1995) 258–262.

PERGAMON

Neuromuscular Disorders 16 (2006) 256–261

www.elsevier.com/locate/nmd

Rapid and accurate diagnosis of facioscapulohumeral muscular dystrophy

Kanako Goto, Ichizo Nishino, Yukiko K. Hayashi *

Department of Neuromuscular Research, National Institute of Neuroscience, National Center of Neurology and Psychiatry (NCNP), 4-1-1 Ogawa-Higashi, Kodaira, Tokyo 187-8502, Japan

Received 10 September 2005; received in revised form 9 January 2006; accepted 18 January 2006

Abstract

Facioscapulohumeral muscular dystrophy (FSHD) is a common muscular disorder, but clinical and genetic complications make its diagnosis difficult. Southern blot analysis detects a smaller sized *Eco*RI fragment on chromosome 4q35 in most facioscapulohumeral muscular dystrophy patients, that contains integral number of 3.3-kb tandem repeats known as D4Z4. The problems for the genetic diagnosis are that southern blotting for facioscapulohumeral muscular dystrophy is quite laborious and time-consuming, and the D4Z4 number is only estimated from the size of the fragment. We developed a more simplified diagnostic method using a long polymerase chain reaction (PCR) amplification technique. Successful amplification was achieved in all facioscapulohumeral muscular dystrophy patients with an *Eco*RI fragment size ranging from 10 to 25 kb, and each patient had a specific polymerase chain reaction product which corresponded to the size calculated from the number of D4Z4. Using southern blot analysis, more than 90% of facioscapulohumeral muscular dystrophy patients have a smaller *Eco*RI fragment than 26 kb in our series, and the number of D4Z4 repeats is precisely counted by this polymerase chain reaction method. We conclude that this long polymerase chain reaction method can be used as an accurate genetic screening technique for facioscapulohumeral muscular dystrophy patients.

Keywords: Facioscapulohumeral muscular dystrophy; Chromosome 4q35; Genetic diagnosis; Southern blotting; PCR; *Eco*RI fragment; D4Z4

1. Introduction

Facioscapulohumeral muscular dystrophy (FSHD) is a common autosomal dominant muscular disorder characterized by its distinct clinical presentation. It often involves weakness and atrophy of facial muscles, followed by shoulder-girdle, the scapula fixators, and the upper arm muscles. Subsequently, pelvic girdle and lower limbs are also affected. About 20% of the patients eventually become wheelchair-bound by 40 years of age [1]. Difficulties of whistling, eye closure, or arm raising are common initial symptoms. Prominent scapular winging and horizontally positioned clavicles are also observed. Facial or shoulder girdle weakness usually appears during adolescence, but signs may be apparent on examination even in early childhood. Asymmetry of muscle involvement is often observed in apparently affected patients, but this is unrelated to handedness [2]. Weakness is relatively mild and the progression is usually slow with frequent association of subclinical hearing loss and retinal vasculopathy. The clinical diagnosis of FSHD is sometimes difficult because the onset of illness and the phenotypic expression is extremely variable, both within and between families [3,4].

The gene locus for FSHD has been identified on chromosome 4q35 wherein an array of tandem repeat units is located. Each repeat is a 3.3-kb *Kpn*I digestable fragment designated as D4Z4 (Fig. 1) [5–7]. The disease is usually associated with a deletion of this repeated region, however the responsible gene has not yet been identified, and the underlying molecular mechanism is still enigmatic. Southern blot analysis using the probe p13E-11 (D4F104S1) [6] is usually performed in the genetic diagnosis of FSHD. Normal individuals have *Eco*RI digested fragments containing D4Z4 repeats which varies from 40 kb to more than 300 kb in size, however, most of the FSHD patients have a smaller sized fragment from 10 to 35 kb. The clinical severity is often correlated to the fragment size, and patients with the smallest *Eco*RI fragment show very early onset and can be associated with epilepsy and mental retardation [8,9].

* Corresponding author. Tel.: +81 42 341 2712; fax: +81 42 346 1742.
E-mail address: hayasi_y@ncnp.go.jp (Y.K. Hayashi).

0960-8966/$ - see front matter © 2006 Elsevier B.V. All rights reserved.
doi:10.1016/j.nmd.2006.01.008

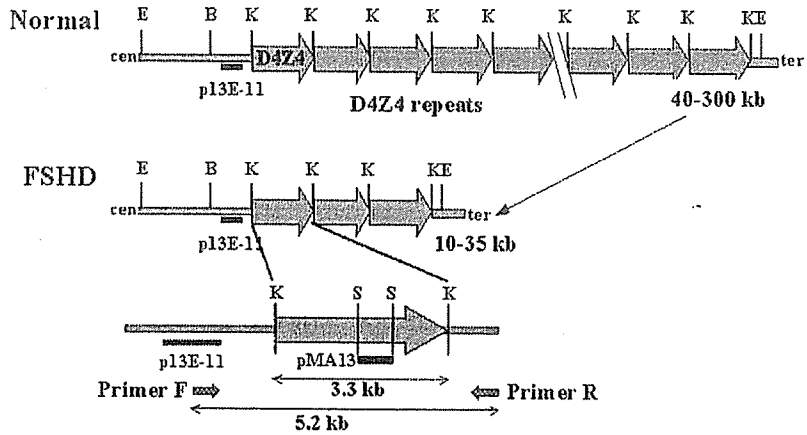

Fig. 1. A schematic diagram of the FSHD gene region on chromosome 4q35 showing the relative locations of primers and the probes used in this study. The primer set has been designed in the non-repeated region, and is expected to produce a 5.2 kb PCR amplified product when template genomic DNA contains one D4Z4 repeat. Cen, centromeric side of the gene; ter, telomeric side of gene; E, *Eco*RI; B, *Bln*I; K, *Kpn*I; S, *Sal*I.

Presently, the accuracy of the molecular diagnosis for FHSD using southern blot is up to 98% [10], however, several factors make this method cumbersome, and more than a week-length of time is required to obtain the results. In the conventional southern blotting method, it is difficult to resolve fragment size over 50 kb, and pulsed-field gel electrophoresis (PFGE) is sometimes taken together to increase resolution. Somatic and germline mosaicism is frequently observed in which more than three different sized *Eco*RI fragments on chromosome 4q are identified [11,12]. Furthermore, homologous 3.3-kb repeat-like sequences are also identified on many other chromosomes such as chromosomes Y and 3p [13,14]. In addition, chromosome 10q26 also contains 3.3-kb *Kpn*I digestable tandem repeats with 98% nucleotide identity to D4Z4 on chromosome 4 [15,16]. Consequently, there is a high incidence of inter-chromosomal exchange between 4q35 and 10q26, which is observed in about 20% of normal individuals [17,18]. In southern blot analysis, the probe p13E-11 used is not specific only to recognize *Eco*RI fragment from chromosome 4q but can also identify *Eco*RI fragment on chromosomes 10q26 and Y. This would require double restriction enzyme digestion using *Eco*RI and *Bln*I to be performed to distinguish 4q35-derived D4Z4 (*Bln*I-resistant) from 10q26-derived repeated units (*Bln*I-sensitive) [19]. From these complexities, there is an urgent need to develop a more simplified and reliable method for the diagnosis of FSHD.

Here, we introduce a new method to count the numbers of D4Z4 repeats on chromosome 4q35 by using long PCR amplification, which is quite useful for the rapid and accurate genetic diagnosis of FSHD.

2. Materials and methods

All clinical materials used in this study were acquired with informed consent. One hundred and five patients with a 4q-linked small *Eco*RI fragment from 10 to 35 kb (Table 3), and seven healthy individuals were examined. Genomic DNA was carefully and gently extracted from blood lymphocytes using a standard method. Southern blot analysis using the probe p13E-11 was performed as previously described [12].

For a long PCR amplification, a 50 μl reaction mixture was used. This mixture contains 400–600 ng of genomic DNA, 25 μl of 2× GC Buffer I (TAKARA BIO INC. Japan), 7.5 μl dATP/dTTP/dCTP mixture (10 mM each), 2.5 μl dGTP/7-deaza-dGTP mix (2:3), 1 μl (10 pM/μl) of each primers, and 0.5 μl (5 U/μl) LA Taq HS (TAKARA BIO). The primers were designed based on the human genomic sequences from GenBank (Accession Numbers D38025 and U74497). The primer sequences are F: 3′-GGCCAGAGTTT-GAATATACTGTGGTCATCTCTGCTCCAG-5′, R: 3′-CAGGGGATATTGTGACATATCTCTGCACTCATC. Amplification was performed using GeneAmp PCR System 9700 (PerkinElmer Japan Co., Ltd, Japan) with the following conditions; 1 min at 94 °C for the initial denaturation, followed by 10 cycles of 10 s at 98 °C and 20 min at 64 °C, and an additional 23 cycles of 10 s at 98 °C, 20 min with autoextension of 20 s per cycle at 64 °C, and 10 min at 72 °C for final elongation. The PCR products were separated by electrophoresis using 0.4% SeaKem HGT agarose gel (FMC BioProducts, ME) in 1× TAE with 0.5 μg/ml ethidium bromide at 3 h. High Molecular Weight DNA Marker (8.3–48.5 kb) (Invitrogen Japan K.K., Japan) and 1 kb plus ladder (Invitrogen) were used. The number of the 3.3 kb *Kpn*I repeated units in the FSHD gene region was calculated by the sequence data from GenBank (Accession Numbers D38024, D38025, and U74497).

In order to ascertain the specificity of the amplified products, we transferred the gels to Hybond N^+ (Amersham Biosciences, Japan) and overnight hybridization at 65 °C was performed with the ^{32}P-labeled probes of p13E-11 and pMA13 (1.3 kb *Stu*I fragment within a D4Z4 unit). The membrane was washed in a stringency of 2× SSC/0.1% SDS for 20 min at 65 °C for two times, followed by

Table 1
Comparison of long PCR and southern blot (SB) analyses

	PCR	SB
Template DNA (μg)	0.4	40
Enzyme digestion	No	*Eco*RI, *Bln*I
Gel size, concentration	11×14 cm, 0.4%	20×20 cm, 0.3%
Required time (h)		
PCR	11	0
Electrophoresis	3	68
Transfer	0	18
Hybridization	0	18
Detection	EB	RI
Total time required	<1 day	7–10 days
Accuracy (%)	90.1[a]	98 [10]

EB, ethidium bromide; RI, radio isotope.
[a] Estimated from the distribution of *Eco*RI fragment size in our series as described in Table 2.

autoradiography for 2 h using BAS2500 image analyzer (Fiji Photo Film, Japan).

3. Results

Table 1 shows the comparison of our newly developed long PCR method and the conventional southern blot analysis. This long PCR method is quite simple, requiring only a small amount of genomic DNA (1/100 of the quantity for southern blotting) and results are rapidly acquired overnight.

The long PCR method amplified five different sized products of 5.2, 8.5, 11.8, 15.1 and 18.4 kb which corresponded to the calculated size from the sequence data of the FSHD region containing one to five D4Z4 repeats, respectively (Fig. 2a, Table 3). These PCR products were not digested by *Bln*I, and were exclusively hybridized by the two probes of p13E-11 and pMA13 (data not shown). The same PCR method was performed on 10 individuals with a small *Eco*RI fragment (from 10 to 25 kb) on chromosome 10q26 but no amplified product was identified (data not shown).

Table 2 shows the distribution of the size of small *Eco*RI fragment on chromosome 4q of 263 FSHD families in our series. Table 3 shows the size of the PCR products, the calculated size of the *Eco*RI fragment, the range of the fragment size detected by southern blot analysis, and number of the patients. A 5.2 kb PCR product that contains one D4Z4 repeat was observed in eight patients with a *Eco*RI fragment from 10 to 11 kb. Sequence analysis confirmed that this 5.2 kb fragment contains one D4Z4 repeat on chromosome 4q35. An 8.5 kb band corresponding to the size with two D4Z4 repeated units was detected in 23 patients with 13–17 kb *Eco*RI fragment. An 11.8 kb product (three D4Z4 repeats) was seen in 26 patients with 16–19 kb fragment, a 15.1 kb fragment (four D4Z4 repeats) was seen in 24 patients with 18–22 kb fragment, and a 18.4 kb product (five D4Z4 repeats) was observed in six patients with 23–25 kb *Eco*RI fragment. The PCR products were amplified from all 87 DNA samples of the patients with an *Eco*RI fragment of 25 kb or less. However, DNA from normal individuals and FSHD patients with larger (≧26 kb) *Eco*RI fragments were not successfully amplified/detected by this long PCR method.

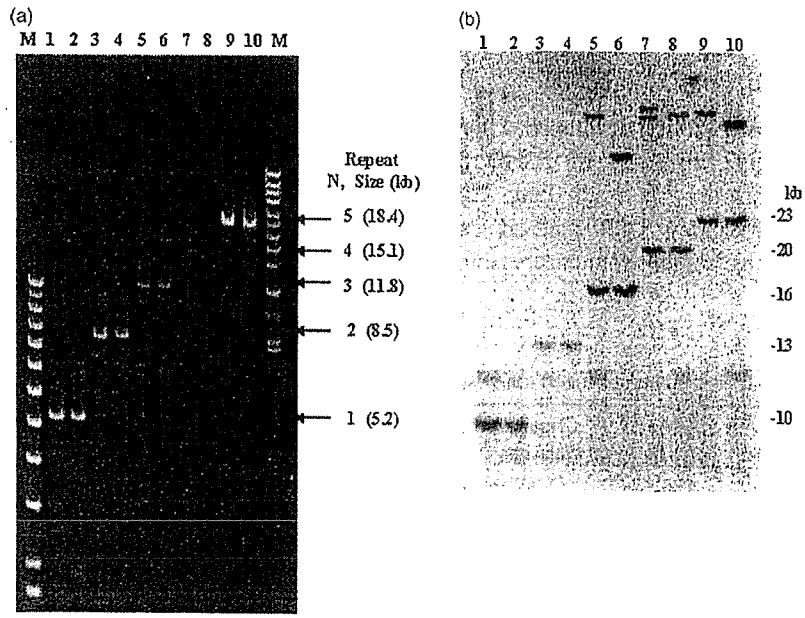

Fig. 2. Long PCR amplification and conventional southern blot analysis using genomic DNA from FHSD patients. (a) A 5.2 kb PCR product was detected on two patients with an *Eco*RI fragment of 10-kb (lane 1), or 11-kb (lane 2) as interpreted from our previous southern blot study. An 8.5-kb band was detected from two patients with a 13-kb (lane 3) or a 14-kb (lane 4) fragment, an 11.8-kb product from two patients with a 16-kb (lane 6) or a 17-kb (lane 7) fragment, a 15.1-kb product from a 20 or a 22 kb fragment, and an 18.4 kb fragment was identified from patients with a 24 and a 25 kb *Eco*RI fragment. These PCR products correspond to the size containing one to five D4Z4 repeated units. (b) Southern blot analysis using the same 10 samples in (a). The samples with the same size of the PCR products showed no difference of the *Eco*RI fragment size, although variable fragment size was previously interpreted.

Table 2
Distribution of *Eco*RI fragment size on chromosome 4q of 263 families in our series

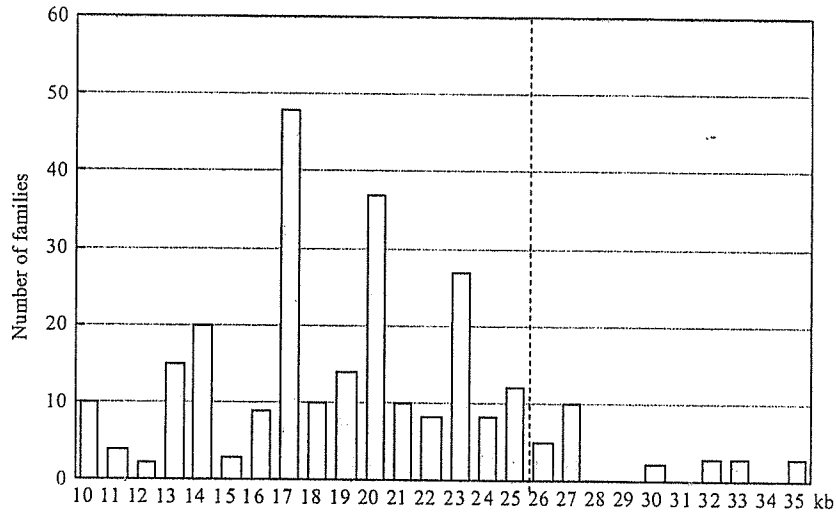

*Eco*RI fragments of <26 kb (dot line) can be amplified by long PCR analysis.

Estimated fragment size from the previous southern blot was not identical among the patients with same numbers of D4Z4 repeats. To determine the inter-individual variability of the fragment size, conventional southern blot analysis was repeated simultaneously. Notably, after the repeated southern blot technique, the *Eco*RI fragment size was similar when the D4Z4 number was the same and this result was consistent with the calculated size (Fig. 2b).

4. Discussions

In this study, we have successfully developed a new method for rapid and specific diagnosis of FSHD by counting the number of D4Z4 repeats via a long PCR amplification technique. This long PCR method can specifically amplify the repeated region from chromosome 4q up to 18.4 kb in size and countable from one to five D4Z4 repeated units.

Table 3
Comparison of the results of long PCR and southern blot (SB) analysis

Number of D4Z4 repeats	PCR product size (kb)	Calculated size of *Eco*RI fragment (kb)	Range of *Eco*RI fragment by SB (kb)	Number of patients examined by PCR
1	5.2	10.2	10-11	8
2	8.5	13.5	13–17	23
3	11.8	16.8	16–19	26
4	15.1	20.1	18–22	24
5	18.4	23.4	23–25	6
6	21.7	26.7	26–35	18 (No amplification)
7	25	30		
8	28.3	33.3		
9	31.6	36.6		

D4Z4 repeat has highly GC-rich sequence up to 73% [20]. Difficulties in PCR amplification often arise when GC content of the template DNA exceeds 50%. This difficulty in PCR amplification was overcame in our study by using thermo-stable long accurate Taq, 7-deaza-dGTP, and a higher denaturing temperature (98 °C) followed by a relatively higher annealing/extension temperature (64 °C) for 20 min with autoextension of 20 s per cycle. Therefore 73% of GC-containing repeated region of more than 18 kb in size was amplified with ease. The specificity of each PCR amplified product was ascertained by several ways. First, both probes (p13E-11 and pMA-13) that were used in the hybridization of the PCR products exclusively recognize fragments containing D4Z4 repeats. Second, the restriction enzyme *Bln*I did not digest the amplified fragments and confirmed that the product is apparently different from the repeats derived from chromosome 10q26, wherein 98% homologous *Kpn*I repeated units and franking sequences are known. Third, this long PCR method did not amplify *Kpn*I repeats from 10q26 even though the only difference is one different nucleotide from each of the primer region on 4q35. We also designed 10q-specific primer set and confirmed that only the 10q-derived repeats could be amplified by using this primer set.

The diagnosis of FSHD is sometimes difficult. Clinical symptoms and severity are quite variable between the patients even within the same family. Up to date, genetic diagnosis of FSHD is solely depended on the southern blot analysis since no responsible gene is yet identified within the candidate region. However, such procedure requires a large amount of DNA and would necessitate at least a week-time period to produce results. The requirement for such

amount of time for analysis dwells on the complexity of the experimental protocols in detecting the various fragments, the sizes ranging from 10 to 300 kb, as well as the determination of the existence of homologous regions on the other chromosomes. Determination of the size of *Eco*RI fragment is important since it is usually correlated to the clinical severity. However, identification of the precise fragment size is often difficult in the conventional southern blotting, since only very low concentrated gels of 0.3% is used to detect large sized fragment, and even minor changes in the experimental conditions would produce different results. In fact, in our very own series, DNA samples containing the same number of D4Z4 repeats showed the same *Eco*RI fragment size on one membrane although the estimated size in our previous analysis detected by different membranes were variable. Therefore, the number of D4Z4 units estimated from the *Eco*RI fragment size using Southern blotting could be misinterpreted from its actual number. From the result of the long PCR analysis, we concluded that the number of D4Z4 is countable from the size of PCR products, and the deletion of the FSHD region is certainly caused by the deleted integral number of D4Z4.

The number of D4Z4 is specifically countable up to five, which corresponds to the estimated *Eco*RI fragment of 10–25 kb in size. When no amplified product was obtained, southern blot analysis is required. In our series, 9.9% of the 4q-linked small *Eco*RI fragments have 26–35 kb as shown in Table 2, but the percentage may be greater in other countries. In the cases having deletion of p13E-11, no product can be obtained in this PCR analysis, since the forward primer is designed within this region. However, considering the complexity of the southern blot technique, this long PCR analysis is useful for the initial screening of the FSHD patients, and also the genetic test for the other family members with a known D4Z4 repeat numbers from 1 to 5 in an index patient. Obtaining accurate results rapidly is always beneficial for the patient, especially during prenatal test. From the economical point of view, PCR analysis is also beneficial since it costs 1/30–40 for the southern blot analysis.

Both primer sequences we used in this study are 4q-specific, and can amplify fragments even those with zero D4Z4 repeat, if any, producing an estimated 1.9-kb product. We also designed a primer set that can specifically amplify the repeated region on chromosome 10q. Theoretically, by using several combinations of these primers, we should be able to distinguish rare cases with short hybrid repeats on 4q or non-FSHD *Bln*I-resistant fragments on 10q. We concluded that the long PCR method could be used as an accurate genetic screening technique for FSHD.

Acknowledgements

We would like to thank Dr Mina Nolasco Astejada (NCNP) for critically reviewing the manuscript. This work was supported by Health and Labor Science Research Grants, Research on Psychiatric and Neurological Diseases and Mental Health, and The Research Grant (17A-10) for Nervous and Mental Disorders from the Ministry of Health, Labour and Welfare, Research on Health Sciences focusing on Drug Innovation from The Japan Health Sciences Foundation, Japan.

References

[1] Lunt PW, Harper PS. Genetic counselling in facioscapulohumeral muscular dystrophy. J Med Genet 1991;28:655–64.
[2] Tawil R, McDermott MP, Mendell JR, Kissel J, Griggs RC. Facioscapulohumeral muscular dystrophy (FSHD): design of natural history study and results of baseline testing, FSH-DY group. Neurology 1994;44:442–6.
[3] Lunt PW, Jardine PE, Koch M, et al. Phenotypic–genotypic correlation will assist genetic counseling in 4q35-facioscapulohumeral muscular dystrophy. Muscle Nerve 1995;2:S103–S9.
[4] Padberg GW, Frants RR, Brouwer OF, Wijmenga C, Bakker E, Sandkuijl LA. Facioscapulohumeral muscular dystrophy in the Dutch population. Muscle Nerve 1995;2:S81–S4.
[5] Upadhyaya M, Lunt P, Sarfarazi M, Broadhead W, Farnham J, Harper PS. The mapping of chromosome 4q markers in relation to facioscapulohumeral muscular dystrophy (FSHD). Am J Hum Genet 1992;51:404–10.
[6] Wijmenga C, Hewitt JE, Sandkuijl LA, et al. Chromosome 4q DNA rearrangements associated with facioscapulohumeral muscular dystrophy. Nat Genet 1992;2:26–30.
[7] Hewitt JE, Lyle R, Clark LN, et al. Analysis of the tandem repeat locus D4Z4 associated with facioscapulohumeral muscular dystrophy. Hum Mol Genet 1994;3:1287–95.
[8] Funakoshi M, Goto K, Arahata K. Epilepsy and mental retardation in a subset of early onset 4q35-facioscapulohumeral muscular dystrophy. Neurology 1998;50:1791–4.
[9] Miura K, Kumagai T, Matsumoto A, et al. Two cases of chromosome 4q35-linked early onset facioscapulohumeral muscular dystrophy with mental retardation and epilepsy. Neuropediatrics 1998;29: 239–41.
[10] Upadhyaya M, Cooper DN. Molecular diagnosis of facioscapulohumeral muscular dystrophy. Expert Rev Mol Diagn 2002;2: 160–71.
[11] Lemmers RJ, van der Wielen MJ, Bakker E, Padberg GW, Frants RR, van der Maarel SM. Somatic mosaicism in FSHD often goes undetected. Ann Neurol 2004;55:845–50.
[12] Goto K, Nishino I, Hayashi YK. Very low penetrance in 85 Japanese families with facioscapulohumeral muscular dystrophy 1A. J Med Genet 2004;41:e12.
[13] Clark LN, Koehler U, Ward DC, Wienberg J, Hewitt JE. Analysis of the organisation and localisation of the FSHD-associated tandem array in primates: implications for the origin and evolution of the 3.3 kb repeat family. Chromosoma 1996; 105:180–9.
[14] Ballarati L, Piccini I, Carbone L, et al. Human genome dispersal and evolution of 4q35 duplications and interspersed LSau repeats. Gene 2002;296:21–7.
[15] Deidda G, Cacurri S, Grisanti P, Vigneti E, Piazzo N, Felicetti L. Physical mapping evidence for a duplicated region on chromosome 10qter showing high homology with the facioscapulohumeral muscular dystrophy locus on chromosome 4qter. Eur J Hum Genet 1995;3:155–67.

[16] van Geel M, Dickson MC, Beck AF, et al. Genomic analysis of human chromosome 10q and 4q telomeres suggests a common origin. Genomics 2002;79:210–7.
[17] Matsumura T, Goto K, Yamanaka G, et al. Chromosome 4q;10q translocations; comparison with different ethnic populations and FSHD patients. BMC Neurol 2002;2:7.
[18] Lemmers RJ, van der Maarel SM, van Deutekom JC, et al. Inter- and intrachromosomal sub-telomeric rearrangements on 4q35: implications for facioscapulohumeral muscular dystrophy (FSHD) aetiology and diagnosis. Hum Mol Genet 1998;7: 1207–14.
[19] Deidda G, Cacurri S, Piazzo N, Felicetti L. Direct detection of 4q35 rearrangements implicated in facioscapulohumeral muscular dystrophy (FSHD). J Med Genet 1996;33:361–5.
[20] Lee JH, Goto K, Matsuda C, Arahata K. Characterization of a tandemly repeated 3.3-kb KpnI unit in the facioscapulohumeral muscular dystrophy (FSHD) gene region on chromosome 4q35. Muscle Nerve 1995;2:S6–S13.

Human Molecular Genetics, 2006, Vol. 15, No. 8 1279–1289
doi:10.1093/hmg/ddl045
Advance Access published on March 10, 2006

Aberrant neuromuscular junctions and delayed terminal muscle fiber maturation in α-dystroglycanopathies

Mariko Taniguchi[1], Hiroki Kurahashi[3], Satoru Noguchi[4], Takayasu Fukudome[5], Takeshi Okinaga[2], Toshifumi Tsukahara[6], Youichi Tajima[7], Keiichi Ozono[2], Ichizo Nishino[4], Ikuya Nonaka[4] and Tatsushi Toda[1,*]

[1]Division of Clinical Genetics, Department of Medical Genetics and [2]Department of Pediatrics, Osaka University Graduate School of Medicine, 2-2 Yamadaoka, Suita, Osaka 565-0871, Japan, [3]Division of Molecular Genetics, Institute for Comprehensive Medical Science, Fujita Health University, Toyoake, Aichi 470-1192, Japan, [4]National Institute of Neuroscience, National Center of Neurology and Psychiatry, Kodaira, Tokyo 187-8502, Japan, [5]Division of Clinical Research, Nagasaki Medical Center of Neurology, Kawatanamachi, Nagasaki 859-3615, Japan, [6]Center for Nano Materials and Technology, Japan Advanced Institute of Science and Technology, Tatsunokuchi, Ishikawa 923-1292, Japan and [7]Department of Clinical Genetics, The Tokyo Metropolitan Institute of Medical Science, Bunkyo-ku, Tokyo 113-8613, Japan

Received October 15, 2005; Revised and Accepted February 28, 2006

Recent studies have revealed an association between post-translational modification of α-dystroglycan (α-DG) and certain congenital muscular dystrophies known as secondary α-dystroglycanopathies (α-DGpathies). Fukuyama-type congenital muscular dystrophy (FCMD) is classified as a secondary α-DGpathy because the responsible gene, *fukutin*, is a putative glycosyltransferase for α-DG. To investigate the pathophysiology of secondary α-DGpathies, we profiled gene expression in skeletal muscle from FCMD patients. cDNA microarray analysis and quantitative real-time polymerase chain reaction showed that expression of developmentally regulated genes, including myosin heavy chain (*MYH*) and myogenic transcription factors (*MRF4*, *myogenin* and *MyoD*), in FCMD muscle fibers is inconsistent with dystrophy and active muscle regeneration, instead more of implicating maturational arrest. FCMD skeletal muscle contained mainly immature type 2C fibers positive for immature-type MYH. These characteristics are distinct from Duchenne muscular dystrophy, suggesting that another mechanism in addition to dystrophy accounts for the FCMD skeletal muscle lesion. Immunohistochemical analysis revealed morphologically aberrant neuromuscular junctions (NMJs) lacking MRF4 co-localization. Hypoglycosylated α-DG indicated a lack of aggregation, and acetylcholine receptor (AChR) clustering was compromised in FCMD and the myodystrophy mouse, another model of secondary α-DGpathy. Electron microscopy showed aberrant NMJs and neural terminals, as well as myotubes with maturational defects. Functional analysis of NMJs of α-DGpathy showed decreased miniature endplate potential and higher sensitivities to *d*-Tubocurarine, suggesting aberrant or collapsed formation of NMJs. Because α-DG aggregation and subsequent clustering of AChR are crucial for NMJ formation, hypoglycosylation of α-DG results in aberrant NMJ formation and delayed muscle terminal maturation in secondary α-DGpathies. Although severe necrotic degeneration or wasting of skeletal muscle fibers is the main cause of congenital muscular dystrophies, maturational delay of muscle fibers also underlies the etiology of secondary α-DGpathies.

* To whom correspondence should be addressed. Tel: +81 668793380; Fax: +81 668793389; Email: toda@clgene.med.osaka-u.ac.jp

INTRODUCTION

Fukuyama-type congenital muscular dystrophy (FCMD; MIM 253800) is an autosomal recessive muscular dystrophy and the second most common childhood muscular dystrophy in Japan, following Duchenne muscular dystrophy (DMD) (1). Clinical manifestations of FCMD include severe congenital muscular dystrophy from early infancy, cobblestone lissencephaly and eye malformation. We previously isolated the responsible gene for FCMD, termed *fukutin* (2,3). Recently, it has been postulated that *fukutin* modulates the glycosylation of α-dystroglycan (α-DG), a major component of the dystrophin–glycoprotein complex (4,5). FCMD is classified as one of the congenital muscular dystrophies, such as laminin-α2-deficient congenital muscular dystrophy (MDC1A) (6). Recently, FCMD has also been classified as a secondary α-DGpathy, as mutations in genes encoding glycosyltransferases result in hypoglycosylated α-DG (7). α-Dystroglycan binds to extracellular matrix proteins such as laminin, agrin and perlecan, which are important in maintaining muscle cell integrity (8). Hypoglycosylated α-DG provokes the post-translational disruption of dystroglycan–ligand interactions in the skeletal muscle of patients, leading to the severe phenotypes of congenital muscular dystrophies (7). Other glycosyltransferases include POMGnT1 (protein *O*-mannose β-1, 2-*N*-acetylglucosaminyltransferase 1), POMT1 and POMT2 (protein *O*-mannosyltransferases 1 and 2), fukutin-related protein (FKRP) and LARGE; mutations in these genes induce human muscle–eye–brain disease, Walker–Warburg syndrome and congenital muscular dystrophy type 1C/1D, and mouse myodystrophy, respectively (9–14).

Primary characteristics of the so-called 'muscular dystrophy' such as DMD include necrotic change and active regeneration of muscle fibers. From infancy, DMD patients usually show dystrophic change in skeletal muscle, accompanied by elevation of serum creatine kinase (CK) levels. However, DMD patients usually maintain their gait until early adolescence. In contrast, FCMD patients show severe phenotypic characteristics from very early infancy, and few patients can acquire gait regardless of serum CK levels (1). Skeletal muscle fibers in FCMD are extremely small, irregular in cell size and architecturally disorganized, and extensive fibrosis prevails from the early infantile stage. However, only a small number of muscle fibers show severe necrotic change or active myofibril regeneration, and satellite cells are also fewer than those of DMD (1,15,16). These phenotypic differences promote the hypothesis that another mechanism may also account for the pathophysiology of secondary α-DGpathies.

Although expression profiling of skeletal muscle from patients with DMD, MDC1A and α-sarcoglycanopathy have been described (17–19), no similar analysis has been reported for FCMD and other secondary α-DGpathies. To investigate the molecular mechanism of FCMD and other secondary α-DGpathies, we profiled gene expression in FCMD skeletal muscle using cDNA microarray and subsequent quantitative real time polymerase chain reaction (PCR). Here we demonstrate that aberrant neuromuscular junctions (NMJs) and maturational delay of muscle fibers are significant to the mechanism underlying secondary α-DGpathies.

RESULTS

Aberrant muscle regeneration is suggested by gene expression profiling of FCMD skeletal muscle

Gene expression profiling of FCMD skeletal muscle was performed using a custom cDNA microarray. Clustering analysis showed similar overall expression profiles of muscle from four FCMD patients, aged 20 days to 1 year, 6 months (Fig. 1A). This similarity is independent of age and histology of the muscle specimen in our samples.

We analyzed individual genes showing distinct expression patterns in FCMD skeletal muscle compared with normal children or DMD patients. Most genes encoding muscle components were down-regulated in FCMD. Among these, *myosin light chain 1, 3* and *4* (*myl1, 3* and *4*) were up-regulated in DMD skeletal muscle, in contrast with FCMD (Fig. 1B). Expression of the developmentally regulated myosin heavy chains (*MYHs*), *MYH1*, *MYH2* and *MYH7* (slow, adult-type), was down-regulated in FCMD but not in DMD, whereas expression of *MYH8* (fast-type) showed no significant change in FCMD compared with DMD or normal controls. Slow-type MYHs (MYH1, MYH2 and MYH7) are present in mature muscle fibers and crucial for sarcomere assembly to maintain muscle integrity, whereas fast-type or developmental MYHs (MYH3, MYH4 and MYH8) are seen in early immature myoblasts or in regenerating fibers. These observations suggest that expression of mature muscle components is suppressed in FCMD skeletal muscle at all ages examined.

With regard to muscle fiber differentiation, myogenic factors including *MyoD*, *myf5* and *myogenin* (*myf4*) showed insufficient signal for the analysis. It is noteworthy, however, that *MRF4* (*myf6*) was down-regulated in FCMD. Expression of the alpha-type cholinergic receptor (*CHRNA*), which is known to be regulated by *MyoD* and *MRF4* (20,21), was much higher in FCMD patients than in normal controls.

We next performed real-time quantitative PCR to further investigate skeletal muscle differentiation. We compared mRNA expression in FCMD muscle with normal or DMD skeletal muscle, as DMD is a good example for active regeneration, in which expression of muscle component and myogenic factor mRNA expression is expected to be up-regulated. Although *CHNRA* was up-regulated in DMD, as predicted, its expression was even higher in FCMD (Fig. 2A and B). Among these cholinergic receptor subtypes, gamma-type cholinergic receptor (*CHNRG*), which is a component of fetal isoforms, was up-regulated, whereas epsilon-type cholinergic receptor (*CHNRE*), which only composes adult isoforms (22), was down-regulated in FCMD (Fig. 2B). MYH slow-type (*MYH7*) was down-regulated in FCMD, consistent with the microarray analysis, whereas expression of fast-type MYH (*MYH11b*) was not altered in FCMD. Interestingly, although *MyoD* and *myogenin* were up-regulated in both DMD and FCMD, *MRF4* was down-regulated in FCMD muscle but up-regulated in DMD (Fig. 2A and B). *MRF4* expression is known to be up-regulated in the late phase of muscle regeneration or differentiation, followed by sequential expression of *MyoD*, *myf5* and *myogenin*, indicating significant roles in terminal differentiation (20,21). These results suggest that FCMD skeletal muscle undergoes an unbalanced differentiation process.

A

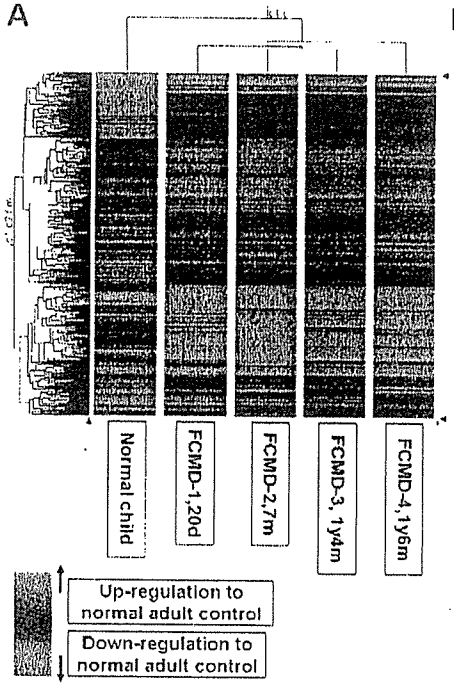

B

gene	FCMD	DMD	Product
myl1	↓	→	myosin light chain 1
myl2	↓	↑	myosin light chain 2
myl3	↓	↑	myosin light chain 3
myl4	↓	↑	atrial /embryonic alkali myosin light chain
myh1	↓↓	↑	myosin, heavy polypeptide 1, adult (slow)
myh2	↓↓	↑	myosin, heavy polypeptide 2, adult (slow)
myh7	↓↓	↑	myosin, heavy polypeptide 7, beta (slow)
myh8	↓	→	myosin, heavy polypeptide 8, (fast)
mybpc1	↓↓	↑	myosin binding protein C, slow type
mybph	↑	→	myosin-binding protein H
actc	↑	↑	actin, alpha, cardiac muscle precursor
actg1	↓	↑	actin, gamma 1
actg2	↓	↑↑	actin, gamma 2
sgcb	↓↓	↓	sarcoglycan, beta
tcap	↓↓	→	titin-cap (telethonin)
ttn	↓↓	↓	titin
des	↓↓	↑	desmin
myf6	↓	→	MRF4 (myf6,herculin)
CHRNA	↑↑	→	nicotinic type, acetylcholine receptor

Figure 1. Cluster image and gene trees from expression profiling of FCMD and normal skeletal muscle. (A) Each line corresponds to the expression signal of each gene. Genes are ordered using the average linkage clustering method to group similar expression profiles. Red denotes up-regulated genes and green denotes down-regulated genes compared with adult control muscle. Note that the expression trends are almost identical within FCMD patients, and FCMD trends are distinct from those of normal children. (B) Expression profile of major muscle components of FCMD and DMD compared with that of normal children. Arrows show the relative expression change (single upward arrow and downward arrow, more than 2-fold increase/decrease; double upward arrows and downward arrows, more than 10-fold increase/decrease; rightward arrow, no change). Note that majority of muscle components are down-regulated in FCMD muscles.

Final maturation step is retarded in FCMD skeletal muscle

To investigate how differentiation is impaired, we examined histological specimens of FCMD skeletal muscle. Marked interstitial tissues with numerous small, round-shaped immature fibers and some necrotic fibers increased with age were seen in FCMD skeletal muscle specimens. Interstitial tissue is prominent from early infancy and progresses with age (Fig. 3A–C), and skeletal muscle from an FCMD fetus also shows rich interstitial tissues (Fig. 3E). Although necrotic change in muscle fibers is not so marked as in DMD fibers, DMD muscle shows less marked fibrosis and more mature fibers, despite more active necrotic and regenerating processes (Fig. 3D). Overall, FCMD muscle is reminiscent of fetal muscle: skeletal muscle from a normal fetus appears rich in fibrous tissues and small, round-shaped immature myotubes (Fig. 3F).

Muscle fiber type is easily identified by ATPase staining. Normally, type 2C fibers are mainly seen in fetal muscle fibers or in regenerating fibers. However, in ATPase-stained cryospecimens, FCMD muscle showed a significantly higher percentage of undifferentiated type 2C muscle fiber contents relative to DMD or control samples ($P < 0.005$) (Fig. 3G and H, Table 1).

Using immunohistochemical analysis, we examined MYH subtypes to confirm the differentiation impairment in FCMD and in myodystrophy mouse (*myd*), which is another model of secondary α-DGpathies. In normal muscle from age-matched controls, no staining of developmental or neonatal MYH (Fig. 3I and J) was seen. In contrast, FCMD and *myd* muscle fibers stained positively for developmental and neonatal MYHs (Fig. 3M and N). These positive fibers corresponded with those staining positive for fast-type MYHs in a serial section (Fig. 3M, O, arrows). Similar staining patterns were observed in skeletal muscle from an FCMD fetus. It is unlikely that all fibers showing developmental MYH expression are derived from regenerating fibers, as few active regenerating or necrotic fibers are seen in the hematoxylin and eosin (HE) specimen at any ages (Fig. 3A–C). Similar staining patterns were observed in skeletal muscles from an FCMD fetus and adult *myd* (data not shown). It is unlikely that all fibers showing developmental MYH expression are derived from regenerating fibers, as few active regenerating or necrotic fibers are seen in the HE specimen (Fig. 3A–C).

These results induce the possibility that maturation might be slowed or arrested in FCMD and *myd* skeletal muscles, and possibly this is common in secondary α-DGpathies. It also

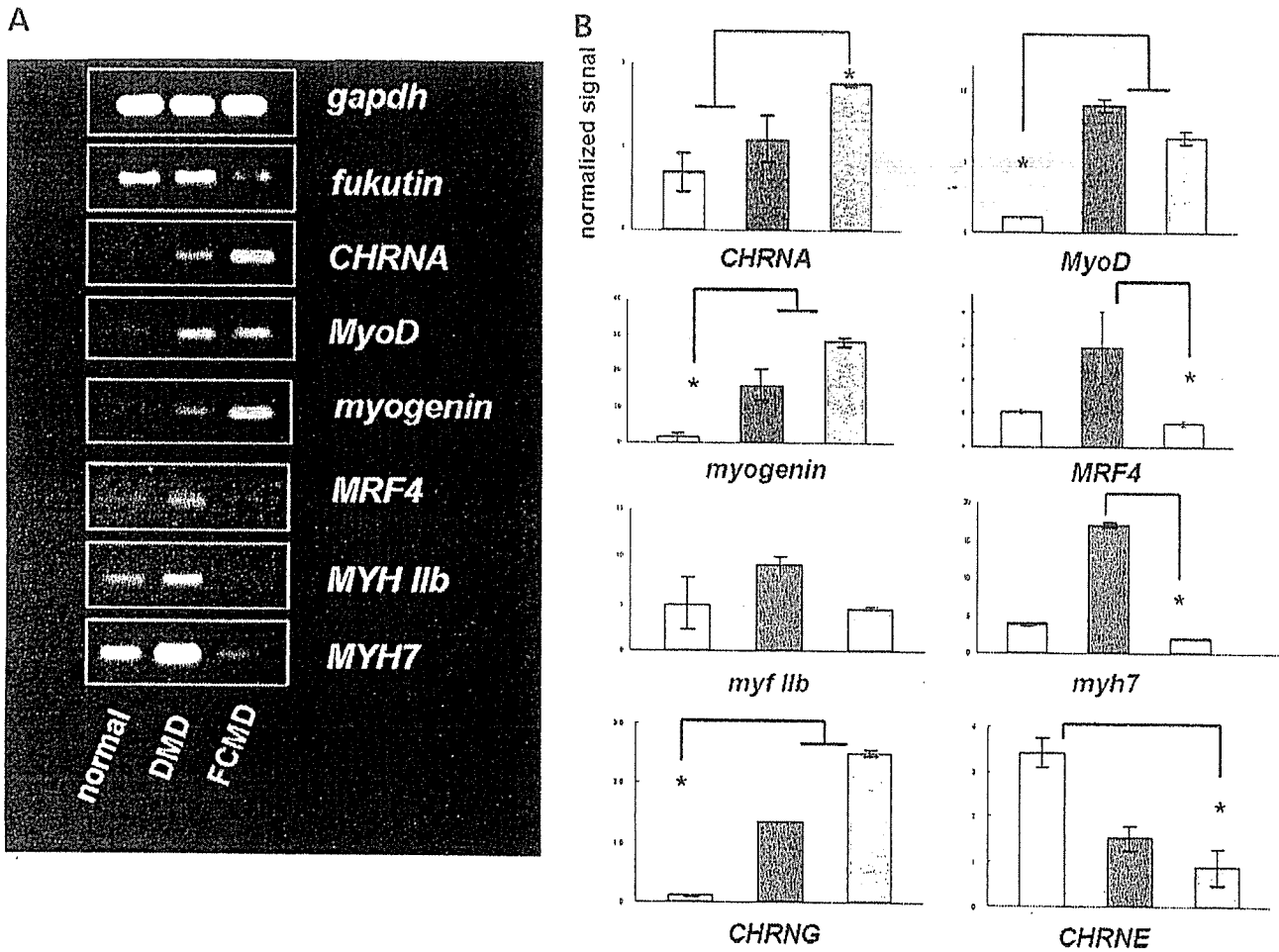

Figure 2. Differential expression of muscle components and myogenic factors in skeletal muscles from FCMD, DMD and normal children. (A) PCR products show that *MyoD* and *myogenin*, which are sequentially expressed in the early phase of muscle regeneration, are up-regulated in DMD and FCMD; however *MYH* and *MRF4* are down-regulated in FCMD but not DMD. (B) Quantitative real-time PCR analysis of mRNA expression. Each bar represents the mean value and 95% confidence interval of duplicate experiments in two patients for each disease and normal control. White bar, normal children; black bar, DMD; gray bar, FCMD. Expression levels are plotted as values normalized to *gapdh*. $^{*}P < 0.005$ (Student's *t*-test).

implies that secondary α-DGpathies have more complex etiology than the so-called 'muscular dystrophy', and that may be partly explained by a maturational defect.

NMJ abnormalities induce maturational delay in secondary α-DGpathies

Microarray analysis showed a reduction in *MRF4* expression in FCMD. Using immunochemistry, we further investigated MRF4 expression in FCMD and in *myd*. Immunoreactivity against MRF4 was reduced dramatically in FCMD muscle fibers (Fig. 4A). In normal skeletal muscles, anti-MRF4 antibody yielded strong signals, which co-localized with the nucleus and NMJs (Fig. 4A, upper columns). MRF4 in FCMD muscles showed weak signals which were not merged with NMJ (Fig. 4A, lower columns). Similar results were obtained in *myd* (data not shown). Regarding the fact that MRF4 is required at the time and place of NMJ development during skeletal muscle differentiation (23), these results prompt the hypothesis that the differentiation process of muscle fibers arrests at this point in secondary α-DGpathies.

We next examined the morphology of NMJs in both FCMD and *myd* by staining acetylcholine receptor (AchR) in NMJs with anti-α-bungarotoxin (Fig. 4B). Almost all the NMJs of FCMD and *myd* showed sparse, weak staining (Fig. 4B, lower columns), in contrast with the dense pattern in normal skeletal muscle (Fig. 4B, upper columns). In normal skeletal muscles, the borders of positive signals were characteristically flared because of multiple layers of synaptic folds, whereas borders in FCMD and *myd* appear smooth and simple, and synaptic folds—particularly secondary folds—were seldom observed. This signal pattern reflects deteriorated or non-deteriorated cluster of AChR on NMJs in secondary α-DGpathies.

Electron microscopic examination of these secondary α-DGpathies revealed aberrant NMJ lesions with abnormal neural endings. NMJs with fewer synaptic folds and secondary clefts were seen in all NMJs of FCMD and *myd* (Fig. 5A–F). In addition, the muscle fibers showed characteristics of immaturity, consistent with our hypothesis that the myotubes are maturationally arrested (Fig. 5G and H). These fibers are distinct from the active regenerating